Universitat Politècnica de Catalunya (UPC)
Universitat Autònoma de Barcelona (UAB)
Universitat de Barcelona (UB)
Institut de Ciències Fotòniques (ICFO)

http://www.photonicsbcn.eu

*Master in Photonics*

## MASTER THESIS WORK

# A bright single photon source: Strong coupling of a single molecule to a plasmonic nano-antenna cavity

**Raúl Izquierdo López**

**Supervised by Prof. Dr. Niek van Hulst, (ICFO) and Nicola Palombo, (ICFO)**

Presented on date 23rd July 2019

Registered at

Escola Tècnica Superior d'Enginyeria de Telecomunicació de Barcelona

# A bright single photon source: strong coupling of a single molecule to a plasmonic nanoantenna cavity

**Raúl Izquierdo López**

Molecular Nanophotonics Group, ICFO - The Institute of Photonic Sciences, Av. Carl Friedrich Gauss, num. 3 08860 Castelldefels (Barcelona), Spain

E-mail: rizqdo@hotmail.com

**Abstract.** Single photon emitters are quantum light sources that can enable a variety of quantum based technologies such as quantum information or quantum random number generation, among others. These single photon emitters can have their brightness increased by coupling to a plasmonic cavity. In this work, this possibility is addressed by spin coating anthracene crystals hosting dibenzoterrylene (DBT) molecules on top of Au dipolar nanoantenna arrays. Thin anthracene crystals covering a big fraction of the nanoantenna arrays were achieved, on which confocal fluorescence microscopy and time correlated single photon counting have been used to characterize the emitters. A time gating based analysis has been used to separate the nanoantenna luminescence from the fluorescence of the DBT molecules, obtaining lifetime values from coupled and uncoupled molecules. A set of 149 coupled molecules and 158 uncoupled molecules was represented in a histogram, showing a distribution from whose mean values the lifetime of DBT molecules ($\tau_0$=4.37 ns) was acquired, as well as a mean lifetime reduction of 2.4 times and a maximum lifetime reduction of 7 times.

## 1. Introduction

Single photon emitters are required as light sources for several applications including noise reduction in measurements of weak absorption, quantum information [1] or high rate quantum random number generation [2] since they provide amplitude-squeezed, indistinguishable photons, which could also be used as propagating qubits. As a result, studies have been made towards the integration of these sources into photonic circuits [3] [4] [5]. In this project, the coupling of single photon emitters to plasmonic nanoantenna cavities is studied with aims to increase the brightness of these sources. This is done by growing thin crystalline films hosting fluorescent molecules on top of nanoantenna arrays. Previously, other approaches have been made to this problem like scanning the emitters with an antenna-tip SNOM (Scanning Near-field Optical Microscope) [6], where enhancement values between 1 and 100 were found depending on the orientation of the emitter. The method used in this work relies on far field measurements though, skipping the complex SNOM tip fabrication process and simplifying the experiment and thus enhancing the success rate.

Single-photon sources, as their name suggests, deliver photons one by one; therefore the probability of measuring two photons emitted by this sources at the same time is negligible. This can be checked by looking for blinking at their timetrace. This blinking consists of short non-emitting periods and can be due to the intersystem crossing to a triplet state, which has a longer lifetime since the triplet-singlet transition is forbidden by the selection rules; this can also be noticed when the molecules photobleaches, as there is no emission after this.

A Hanbury-Brown-Twiss (HBT) experiment represents another way of identifying single photon sources by measuring the second order correlation between photons emitted by the same

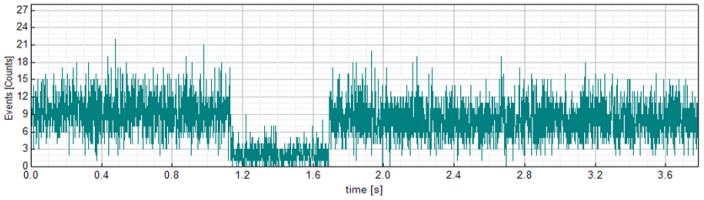


(a)

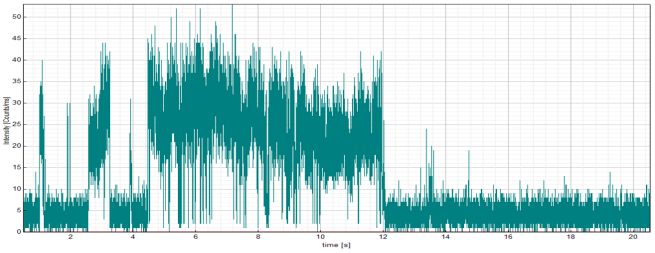

(b)

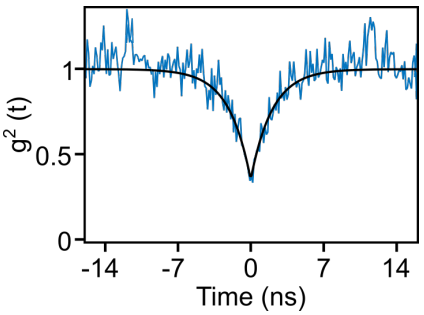


(c)

**Figure 1.** (a) Timetrace of a blinking single molecule. (b) Timetrace of a single molecule photobleaching after some blinking. (c) HBT experiment performed on a hBN defect. $g^{(2)}(0) < 0.5$, meaning that this is a single photon emitter.

source with a certain delay ($g^2(\tau)$). If the source is a single-photon one, then the probability of detecting more than one photon at 0 time delay must drop to 0.

$$g^{(2)}(\tau) = \frac{\langle I(t)I(t+\tau)\rangle}{\langle I(t)\rangle^2} \tag{1}$$

Several kinds of single photon sources can be found, like radiative defects in solid state systems (N vacancy centers in diamond or defects in 2D materials as hBN or $WS_2$), trapped single atoms or single molecules. In this project, the studied source consisted on single organic molecules embedded in an organic anthracene crystal. The chosen molecule was dibenzoterrylene (DBT), which has been found to possess a great photostability at room temperature, with a single molecule providing around $10^6$ photons per second and more than $10^{12}$ photons before photobleaching as well as a quantum yield near 1, which makes it a good candidate for a bright single-photon source. Moreover, the anthracene crystal as a host helps decreasing the drift of the emitters during the measurements and protects the molecules from oxygen quenching, resulting in an increase of the photostability. Previous studies have also determined that the electric dipole moment of DBT molecules in anthracene is oriented parallel to the substrate ("in plane oriented") [7].

A single photon emitter on its own spontaneously emits photons at a certain rate $\Gamma_0$ after being excited. This rate can be modified by placing the emitter near to an optical cavity, which would have a decay rate $\kappa = \frac{\omega_0}{Q}$ where Q is the quality factor of the cavity. The coupling between the emitter and the cavity can be quantified through the coupling strength, defined as

$$g(\vec{r}, \hat{e}, \omega) = \frac{1}{\hbar}\vec{\mu} \cdot \vec{E}(\vec{r}, \hat{e}, \omega) \tag{2}$$

where $\vec{\mu}$ is the dipole moment of the emitter and $E = \sqrt{\frac{\hbar\omega}{2\varepsilon_r\varepsilon_0 V_m}}$ is the electric field of a photon of frequency $\omega$ inside the cavity, where $\varepsilon_r$ is the relative permittivitty, $\varepsilon_0$ is the vacuum permittivitty and $V_m$ is the mode volume of the cavity. This quantity can be compared to the decay rates of the emitter and the cavity loss rate, leading to 2 different regimes. If g>> $\Gamma_0, \kappa$ the system is said to be strongly coupled, as the energy is transferred many times between

the emitter and the cavity before the dexcitation. This has been achieved in high Q dielectric cavities, but their low $\kappa$ prevents these systems from being very bright sources. On the other hand, in the weak coupling regime the energy is transferred from the emitter to the cavity but not in the opposite way ($\kappa > g >> \Gamma_0$), specially in the so called bad cavity regime ($\kappa >> g >> \Gamma_0$) where the emission, which is produced through the cavity mode, has its rate increased due to the high cavity losses.

Plasmonic cavities appear as good choice for several reasons. First, the cavity mode volume ($V_m$) in a nanoantenna is much smaller than the wavelength, thus by placing an emitter in a way so it overlaps with the cavity mode, the coupling strength can be significantly increased. Second, plasmonic cavities are way lossier than dielectric ones because of ohmic loss, with quality factors usually between 5 and 20. However, the loss is mostly radiative in the plasmon mode. Because of this, plasmonic dipolar antennas seem to be a good cavity to enhance the brightness of single emitters through weak coupling.

Following Fermi's golden rule, the probability of an emitter to produce a photon depends not only on the element in the hamiltonian that relates the initial and final state, but also on the density of states at the photon energy, which is strongly affected by the photonic environment of the emitter [8] [9].

$$\Gamma_{i\to f} = \frac{2\pi}{\hbar} |\langle f| H |i\rangle|^2 \rho(\hbar\omega) \tag{3}$$

Thus, a change in the photonic environment of an emitter affects the lifetime of its excited state through a change in the density of states, which is known as Purcell effect. Moreover, by positioning the emitter close to an environment resonant at the transition energy as a metallic dipole antenna, the density of states of the excited state is increased [10] and so is the decay rate. As a consequence, measuring the lifetime (inverse of the decay rate) of single emitters with and without a plasmonic cavity can be used to quantify the coupling between the emitter and the cavity.

## 2. Methods

### *2.1. Nanoantenna cavities*

As a cavity, Au rod nanoantennas were used with the purpose of obtaining a $\lambda/2$ dipole antenna. These antennas were distributed in sweep arrays, that is, a matrix of antennas were the length changes along one of the directions while keeping constant the other properties. Each antenna was made of gold on top of a titanium layer by electron beam lithography on a glass substrate, has a width of 50 nm and a length varying between 40 nm and 200 nm. The separation between antennas was 2 $\mu$m.

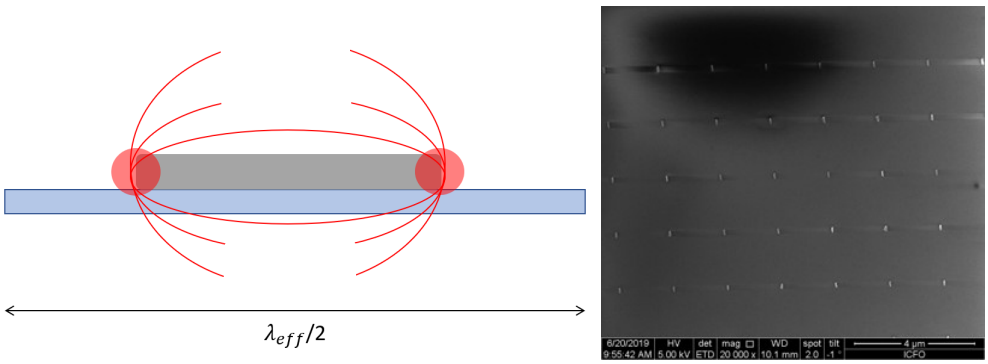


(a) (b)

**Figure 2.** (a) Sketch of a $\lambda/2$ dipolar nanoantenna showing two hotspots at its ends. (b) SEM image of the nanoantenna arrays.

*2.2. Single molecule samples fabrication*

In order to grow the films, first a solution of anthracene in diethyl ether 2.5 mg/ml was prepared, to which 10 $\mu$l/ml of benzene were added. Then, a 2 $\mu$M solution of DBT in toluene was diluted in the previous one with 3% in volume concentration. This final solution was spin coated on top of the substrate, which was a glass cover slide with the Au nanoantenna arrays on top. In the spin coating process 15 $\mu$l of the solution were casted on the substrate, which was spinning at 2000 RPM for 25.5 s. After performing the required measurements, the nanoantenna arrays were washed in acetone, water and methanol, so they could be reused again. Other variations in this process were attempted as different rotation speeds, plasma etching or vacuum evaporation in order to reduce the thickness of the crystals.

*2.3. Characterization*

Once the samples were fabricated, they were optically characterized. First of all, right after the fabrication process, the samples were observed in an optical microscope in order to see whether the anthracene crystals had grown on top of the arrays. Once it was verified, an inverted confocal microscope as the one described in the figure 3 was used to study the sample through several different measurements.

As excitation source, a tunable pulsed fiber laser is used at a wavelength of 750±5 nm, followed by a 660 nm long pass filter. After this, the excitation light passes the shutter and, after being focused by a NA=1.3 oil immersion objective, shines the sample which is mounted on a piezoelectric stage that allows to scan the sample in the 3 dimensions. Fluorescence is then collected in reflection by the same objective and passes through a detection 780 nm long pass filter to cut the laser radiation so only the emission from the sample is collected. Finally, a 50:50 beam splitter separates light in two different paths to make it arrive to 2 fast APD's that are connected to a Time Correlated Single Photon Counting (TCSPC) module. Alternatively, a mirror can be placed in the optical path to send light to a EMCCD camera used as a spectrometer instead of the APDs.

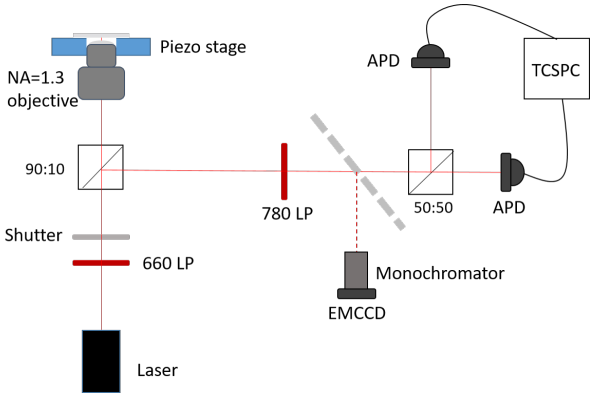


**Figure 3.** Setup for optical characterization of the samples by confocal fluorescence microscopy.

First information that we can extract by studying the sample are microscope images by switching the excitation source to a white light lamp and directing the collected light to a camera. A second measurement that can be done is the fluorescence of the sample. After exciting the sample, light was directed to the APDs. By recording the number of photon counts in each spot while scanning the sample, a fluorescence image of it can be obtained. As the laser spot has a size of ∼300 nm, the step size of the scan was set to be 200 nm, which allowed to obtain an image with 200 nm pixel size.

By removing the detection filter and lowering the power to prevent the APDs from saturating, images can be made from the measurement of the reflected laser radiation on the substrate, which gives qualitative information about the topography of the sample thanks to the contrast existent between anthracene films of different heights.

By changing the path of the collected light, it can be made to arrive to a EMCCD camera, which acts as a spectrometer. With this, the spectrum of the collected light can be measured at a single spot or, by scanning the sample, a spectral map can be obtained with a spectrum at each pixel.

Finally, the TCSPC modules are used to measure the delay between the excitation pulse and the detected photons and plot this data in histograms that represent the decay of the emitter's excited state, allowing to retrieve its lifetime. For these measurements, the repetition rate of

the laser was set to 39 MHz to let the sample decay between pulses. An issue to be taken into account in this section is the time duration of the measurement, since the experimental setup suffers from drift leading to defocusing after long time periods. Obtaining a good signal to noise ratio in the TCSPC histogram depends mainly of two parameters: the incident laser power and the integration time in each pixel. Increasing both parameters increases the number of experimental data but the latter limits the size of the maps that can be obtained without compromising the measurements due to drift. Thus, increasing the laser power will allow to obtain better histograms without increasing the measuring time. However, this parameter is also limited by the maximum power the nanoantennas can receive without melting. After studying this limit, the optimal configuration was found to be using 100 $\mu$W pump while setting the timebin to 1.5 s per pixel. This allowed to record images up to 17 $\mu$m x 17 $\mu$m with a step size of 200 nm/px. Note that scans with such sizes take several hours to be carried out.

*2.4. Data analysis*

When combining the TCSPC measurements with a scan, a photon histogram is obtained in each one of the pixels of the image. In the case of a coupled molecule, two exponential decays will contribute to the photon histogram: one due to the convolution of the Instrument Response Function (IRF) of the system and the nanoantenna luminescence (since the nanoantenna luminescence is faster than the IRF) and one another due to the molecule. Since the molecule, coupled or not, will have a slower decay than the other contributions (see figure 4), time gating is proposed as a method to analyse the data. This consists in taking into account photons in a certain interval of time for the analysis. The interval between 2 ns and 25 ns after the excitation has been found to allow to separate the photons coming from the antennas from the ones emitted by the molecules. Then, this data can be fit by a single exponential that represents just the decay of the molecules.

Hence, the process followed to obtain lifetime data was the following: using time gating analysis, an image integrated in the first 0.8 ns (where the nanoantenna luminescence dominates) was compared to another image integrated between 2 ns and 25 ns (where the contribution from the nanoantennas had disappeared so only molecules are depicted). In case both a molecule and a nanoantenna overlapped, the TCSPC histogram was examined and, if the signal to noise ratio was high enough, it was fitted to a single exponential decay between 2 and 25 ns. This analysis was done on a total of 30 images varying in size from 6 $\mu$m x 6 $\mu$m to 17 $\mu$m x 17 $\mu$m.

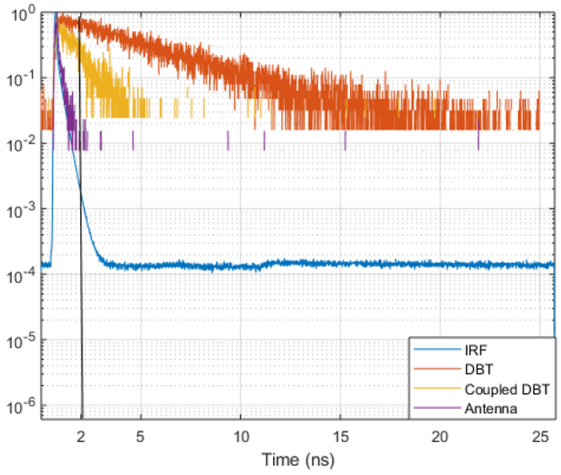


**Figure 4.** Comparison of the photon histograms corresponding to the IRF and measurements on an antenna, a coupled molecule and an uncoupled molecule. A vertical line is drawn at 2 ns to show that the antenna contribution is negligible in the 2-25 ns interval. All values have been normalized to the maximum value of the histogram.

## 3. Results and discussion

### *3.1. Single molecule sample fabrication*

Several approaches were considered in order to cover large areas of the nanoantenna arrays with a thin anthracene crystal containing DBT molecules. The first one of these was to optimize the conditions of the spin coating process. In this way, several rotation speeds were tried and, as reported in other works [11], the obtained crystal flakes are thinner the higher the rotation speed is. Nevertheless, the lateral size of these flakes also decreases when increasing the rotation speed. Because of that, a compromise between the thickness and the lateral size of the flakes was found at 2000 RPM. It was also determined that the optimal way to cast the solution is while the substrate is already spinning. Variations of the solution proposed in the methods section were tested, where the concentration of anthracene was set to twice and half of the one stated. Neither of these variations showed significantly different results.

Thereafter, other strategies were tested to reduce the thickness of the resulting crystals after the spin coating. One of these consisted on attacking the crystal by means of a plasma etching process. Two different gases were used to create the plasma: He and Ar. He ions are lighter than Ar ions, so the process is less aggressive at the surface but the He ions have a higher penetration. As this is an aggressive process for an organic crystal as anthracene, the conditions were set to cause the minimum etching possible (1 W, RF power, 1 mTorr gas pressure and 1 s exposure time) on a sample fabricated at 1000 RPM (thicker crystals than at 2000 RPM). Similar results were found with both gases: most of the surface of the crystal was etched away, along with small holes appearing on the substrate. In initially thin flakes, this process removed most part of the material, while the relative decrease in thickness was lower for the thicker part of the flakes. This resulted in a reduction in the number of thin flakes while maintaining the thick flakes.

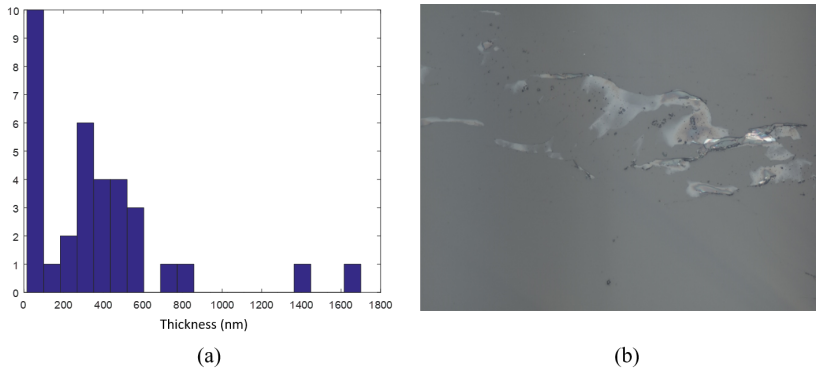


**Figure 5.** (a) Histogram representing the thickness crystal of anthracene crystals, measured with a profilometer after Ar plasma etching. Note that a big fraction of the flakes have a thickness below 100 nm, but still most of the crystals have a thickness above 100 nm. (b) 50x microscope image of a flake. By the contrast with the background, it can be seen that the thickest parts of the flakes remain.

Then, the optical properties of the sample were studied to see if the molecules still had fluorescent emission. The emission of the molecules was followed in time, showing that there were still photostable molecules after the plasma etching, but the fraction of unstable molecules had increased, especially in the thinnest parts of a flake. The drastic reduction in the surface of the thin flakes while maintaining thick flakes shows that this process is not adequate for the experiment carried out in this project.

Another method thought to decrease the thickness of the crystals was letting them sublimate at room temperature. Furthermore, to speed up this process, the samples were left in vacuum to avoid vapour saturation. Optical microscope images showed that, while the thickness was slightly reduced, the lateral size of the flakes reduced drastically, meaning that this approach

was not suitable to cover large areas of the arrays. In the figure 6, microscope images of the anthracene crystals are shown immediately after spin coating and after 19 hours in vacuum.

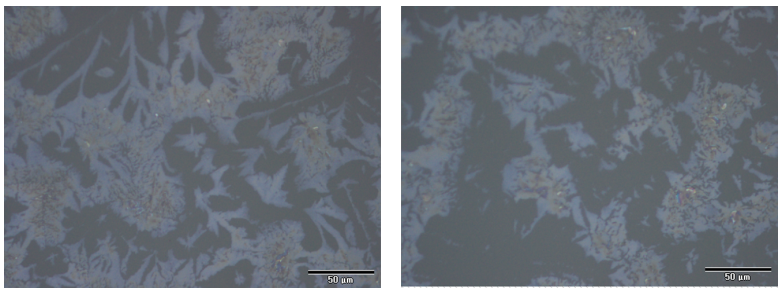

**Figure 6.** Anthracene crystals right after spin coating (left) and after 19 hours sublimating in vacuum (right). Note the significant reduction in the surface of the flakes by looking at the size of the blank spaces between them.

*3.2. Measurements on DBT molecules in nanoantenna cavity*

In order to perform the measurements on the arrays, several tasks had to be carried out to characterize the DBT molecules. First of these was finding the optimal pump wavelength, which turned out to be at 750 nm. Using this excitation wavelength the molecules were brighter while the background noise remained the same, resulting in a better signal to noise ratio. Then, using this pump wavelength, the spectrum of a DBT molecule was measured (figure 7(a)). Note that the measured spectrum has been modified by the detection filter (760 long pass).

Another feature of DBT molecules that can be of interest before measuring on the nanoantennas is the TCSPC histogram of the DBT molecule, so both its shape and its typical lifetime values are known to make the analysis of photon histograms from coupled molecules easier. This is shown in figure 7(b) along with a single exponential fit.

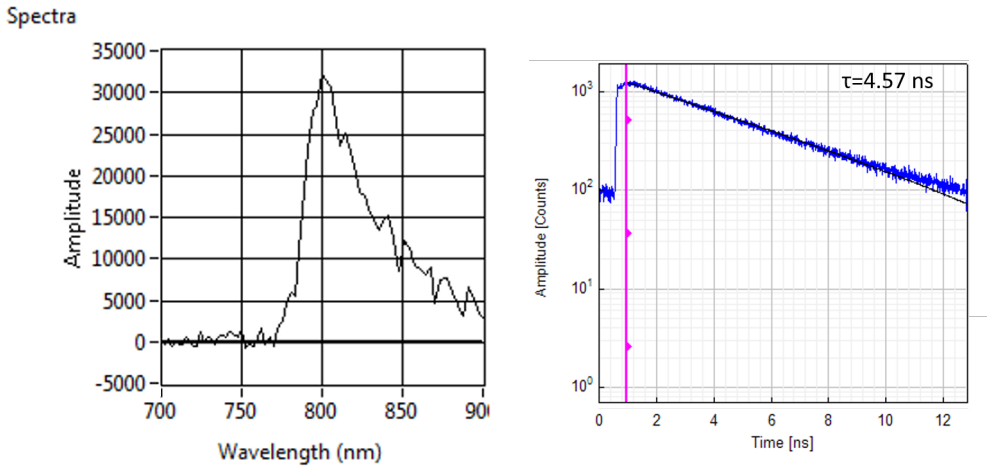


(a) (b)

**Figure 7.** Measurements done to characterize the sample. (a) Measured spectrum of a DBT molecule after the detection 760 long pass filter. (b) TCSPC histogram of a DBT molecule (in blue) and single exponential fit (in black) giving a lifetime value of 4.57 ns.

Thereafter, a complete set of measurements including camera, fluorescence and laser reflection images, as well as spectral maps and lifetime maps can be obtained. In the figure 8, a set of the first three measurements mentioned is shown. These can be used to decide whether the crystal's thickness and surface covering the arrays are adequate to perform measurements.

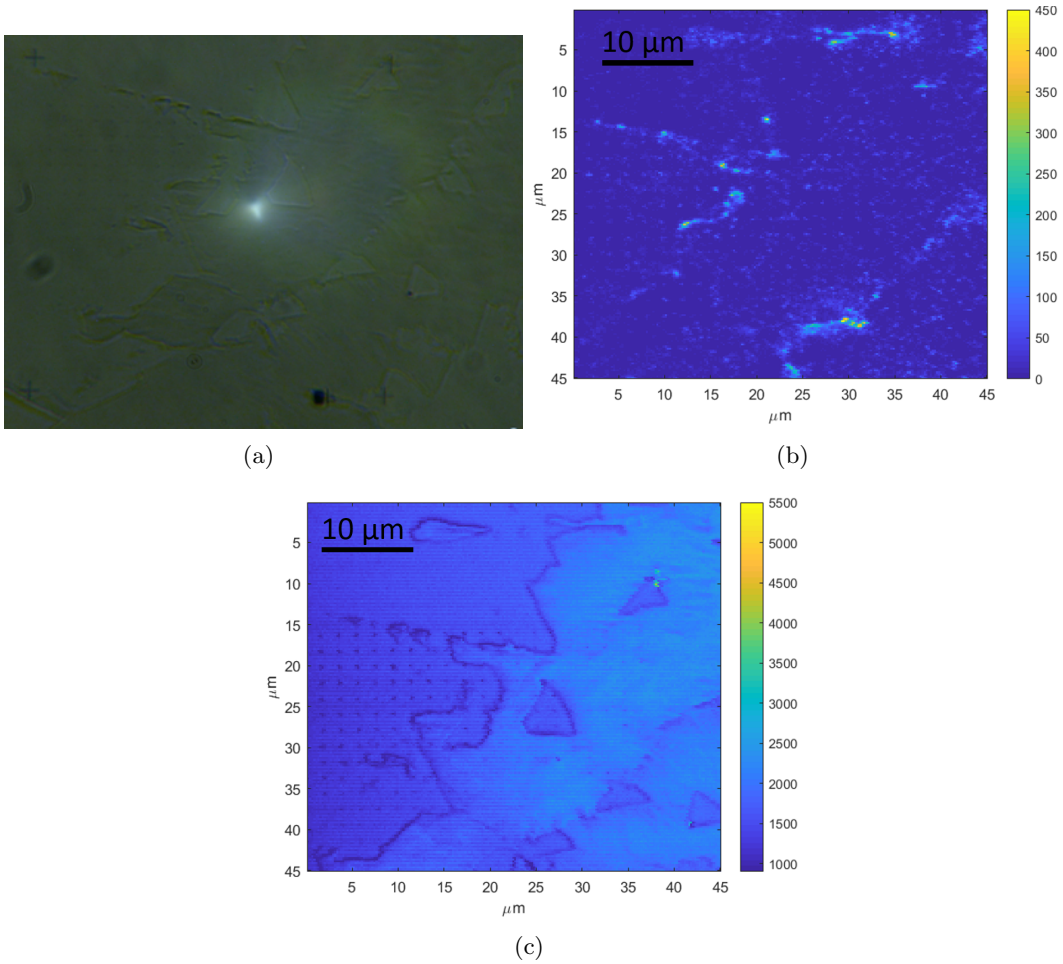


(a) (b) (c)

**Figure 8.** (a) Image taken with the camera connected at the microscope under white light illumination. (b) Fluorescence image after exciting the sample with 100 $\mu$W laser radiation in the band 750±5 nm using a 660 long pass excitation filter and a 760 long pass detection filter. (c) Laser reflection image of the sample. The contrast between the background and the flakes is a good indicator of the height differences.

In the figure 8 it can be seen that the crystal has a very big surface which allows to cover a relevant fraction of the antenna array. By looking at the subfigure (b) two conclusions can be drawn: first, that the molecules tend to agglomerate at the edges of the flake (this was continuously observed in every experiment) and second, that in the inside of the crystal the density of molecules offers enough overlapping cases with antennas but still is low enough to avoid exciting too many molecules at once. This is also related to the fact that crystals are wide enough to prevent the edges to be near between them, which would increase the concentration of DBT molecules. This fact is important for TCSPC measurements, as if several molecules are excited and only one is coupled (the uncoupled ones can be in the opposite edge of the ∼300 nm spot or even in a different plane) the sum of the TCSPC histograms will be a histogram with a longer lifetime than the one that the uncoupled molecule actually has, even if it is still shorter than the lifetime of a DBT molecule alone. Also, by looking at the contrast in subfigure (c) it can be stated that the flake is almost flat in most of its surface.

In figure 9 the different stages in the process of obtaining lifetime maps of the samples are shown. By comparing the subfigures (a), (b) and (c) it can be easily seen that the time gating technique works in separating the nanoantennas luminescence from the DBT molecules emission. In subfigure (d) a lifetime map is represented. However, when looking at the TCSPC histogram of the high lifetime (8-9 ns) spots, it was seen that such high values were due to a

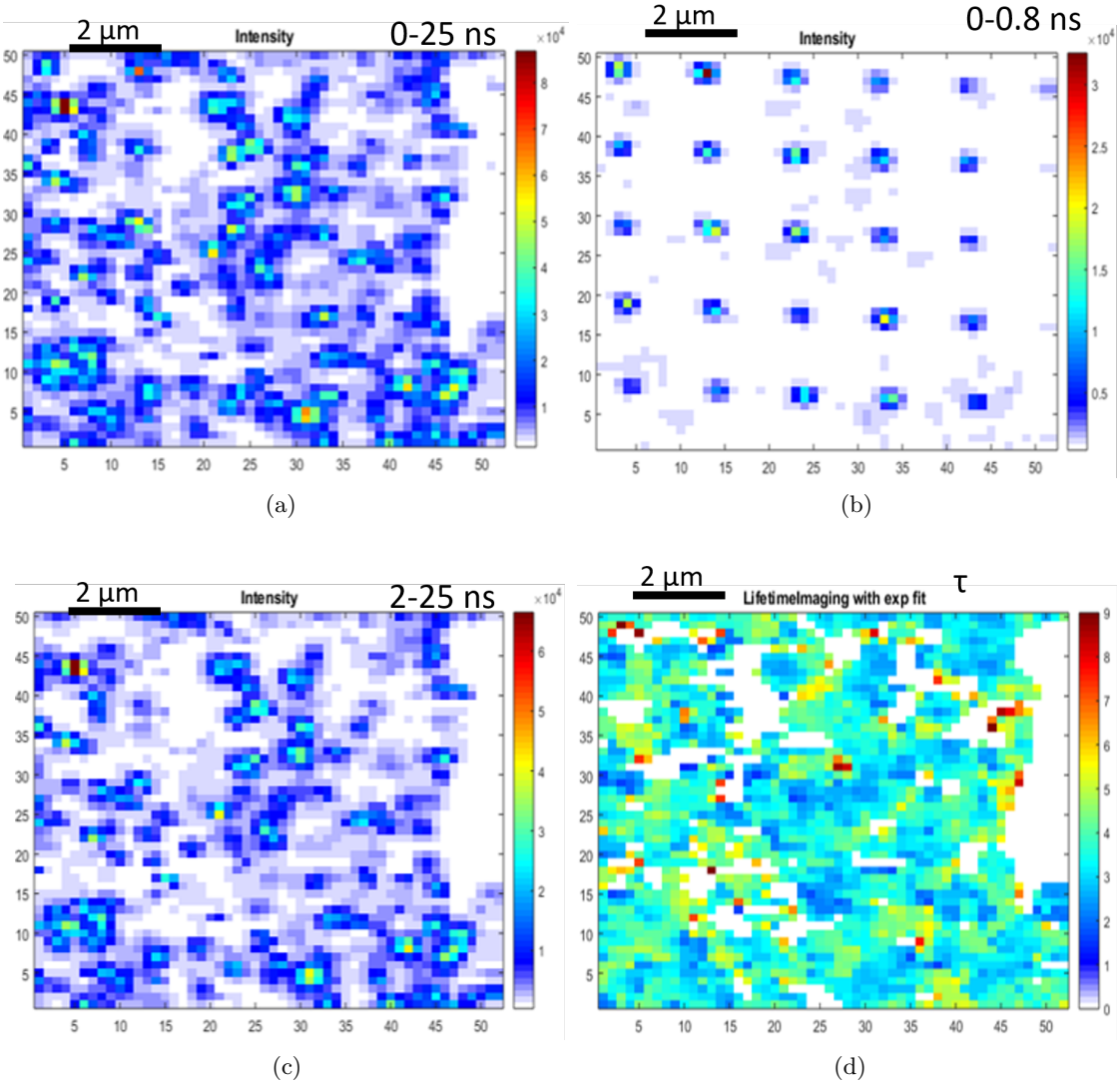


**Figure 9.** (a) Intensity (in photon counts) integrated over all the time interval between pulses. (b) Intensity (in photon counts) integrated only over the first 0.8 ns. Only the antennas remain visible as they are the dominant contribution in this interval. (c) Intensity (in photon counts) integrated between 2 and 25 ns. The antennas no longer emit in this interval, so only the molecules are seen. (d) Lifetime (in ns) map of the sample after a single exponential fit on the data integrated between 2 and 25 ns.

bad fitting caused by not having a sufficient amount of photons. This map was analysed as explained in the methods section, extracting the lifetime values of both coupled and uncoupled molecules, which are shown in the figure 10.

To make the histograms represented in figure 10, the coupled molecules were defined as those which were near a nanoantenna (less than 200 nm away) and with a lifetime value below 3 ns. The rest of the molecules fell under the category of uncoupled. The results show that there is actually coupling between the DBT molecules and the nanoantennas. The measured mean lifetime out of 149 coupled molecules was 1.84 ns and that out of 158 uncoupled ones was 4.37 ns, giving a mean of 2.38 times lifetime reduction. Furthermore, the shortest lifetime measured was 620 ps, which compared to the mean lifetime of the uncoupled molecules gives a 7 times maximum lifetime reduction. Note that the width relative to the mean value is larger for the coupled molecules, this is due to the different degree of coupling between the molecules and the nanoantennas as a consequence of variations in the distance between them. Moreover, the 4.8

ns lifetime value reported in [7] falls within the uncoupled molecule histogram.

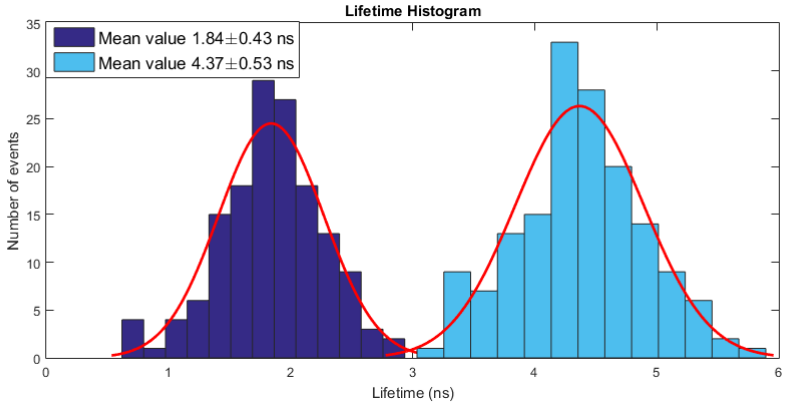


**Figure 10.** In dark blue, histogram representing the lifetime values obtained for coupled molecules, out of a total of 149. The mean value is 1.84±0.43 ns. In light blue, histogram representing the lifetime values obtained for uncoupled molecules, out of a total of 158. The mean value is 4.37±0.53 ns.

## 4. Conclusions

It has been demonstrated that the fabrication of anthracene crystals hosting DBT molecules on top on nanoantenna arrays is possible, obtaining flakes with enough surface to cover large portions of the nanoantenna arrays, which are also thin and flat enough to allow the possibility of measuring coupling between the DBT molecules embedded in the crystal and the nanoantenna cavities.

Furthermore, these DBT molecules have been optically characterized through fluorescence measurements, obtaining both their spectrum (limited by the filters in the setup) and their lifetime, which is in agreement with values previously reported.

Moreover, the coupling between the single photon emitters and the cavities has been studied by means of lifetime measurements, which have given out values of 2.4 times mean lifetime reduction and 7 times maximum lifetime reduction, in agreement with what was expected.

## References


[1] Lounis B and Orrit M 2005 Single-photon sources *Rep. Prog. Phys.* **68** 1129-1179

[2] Rarity J G, Owens P C M and Tapster P R 1994 Quantum random-number generation and key sharing *Journal of Modern Optics* **41** 2435-2444

[3] Lombardi P, Ovvyan A P, Pazzagli S, Mazzamuto G, Kewes G, Neitzke O, Gruhler N, Benson O, Pernice W H P, Cataliotti F S and Toninelli C 2018 Photostable molecules on chip: integrated sources of nonclassical light *ACS Photonics* **5** 126-132

[4] Kewes G, Schoengen M, Neitzke O, Lombardi P, Schönfeld R S, Mazzamuto G, Schell A, Probst J, Wolters J, Löchel B, Toninelli C and Benson O 2016 A realistic fabrication and design concept for quantum gates based on single emitters integrated in plasmonic-dielectric waveguide structures *Scientific Reports* **6**

[5] Zadeh I E, Elshaari A W, Jöns K D, Fognini A, Dalacu D, Poole P J, Reimer M E and Zwiller V 2016 Deterministic integration of single photon sources in silicon based photonic circuits *Nano Lett* **16** 2289-2224

[6] Singh A, Calbris G and van Hulst N F 2014 Vectorial nanoscale mapping of optical antenna fields by single molecule dipoles *Nano Lett* **14** 4715-4723

[7] Toninelli C, Early K, Bremi J, Renn A, Götzinger S and Sandoghdar V 2010 Near-infrared single-photons from aligned molecules in ultrathin crystalline films at room temperature *Optics Express* **18** 6577-6582

[8] Hugall J T, Singh A and van Hulst N F 2018 Plasmonic Cavity Coupling *ACS Photonics* **5** 43-53

[9] Singh A, de Roque P M, Calbris G, Hugall J T and van Hulst N F 2018 Nanoscale mapping and control of antenna-coupling strength for bright single photon sources *Nano Lett.* **18** 2538-2544

[10] Purcell E M, Torrey H C and Pound R V 1946 Resonance absorption by nuclear magnetic moments in a solid *Phys. Rev.* **69** 37

[11] Wu Y L 2007 Control over colloidal crystallization by shear and electric fields (Doctoral dissertation) University of Utrecht